Measurement 203 (2022) 111960

Contents lists available at ScienceDirect

Measurement

journal homepage: www.elsevier.com/locate/measurement

Modelling and testing the measurement repeatability of linear and angular positions of a measuring arm (miniature NaviFAST 6D DEVICE)

Agnieszka Kobierska *, Piotr Rakowski, Leszek Podsędkowski

Institute of Machine Tools and Production Engineering, Lodz University of Technology Stefanowskiego 1/15, 90-924 Lodz, Poland

ARTICLE INFO

Keywords:
Measuring arm
Modelling
Accelerometer
Gravity
Repeatability

ABSTRACT

This paper presents the use of a 6 DoF position measurement method with the NaviFast6D device, which is a short-range measuring arm for linear and angular position measurements. The device is used in the measurement of correct hip prosthesis fixation during hip surgery. The arm is equipped only with accelerometers, which is an innovative application that needs to be verified. The described experimental tests of determining the repeatability of the NaviFast6D demonstrated the correctness of the method. The analysis of the measurement repeatability limitations in the measurement and the dependence of the measurement repeatability on the arm base position, was described in detail. The need for about 400 repetitions of the measurement to obtain repeatability of measurement averaged in the range of 0,1 ÷ 0,2 mm was demonstrated. The applicability of the measuring arm in the case of approaching to the vertical of any axis of the arm joints was determined.

1. Introduction

Today's measurement technology is aimed at providing data for process supervision with regard to quality of measurement at the highest possible level. An example of such devices are coordinate measuring arms and their application in production measurements. Verification of geometric parameters of objects in 3D space is one of the main tasks of coordinate measuring arms [1,2]. This is due to the high quality requirements of manufactured products checked in this respect already at particular technological stages. A similar situation occurs in medical geometric measurement (especially in orthopedics), where reliable measurement information is linked to correctly performed surgery and the well-being of the patient after the procedure. Both of the discussed examples are characterized by the possibility of a limited number of measurements of the same parameter, often the measurement is performed once. This raises the question of what the uncertainty and repeatability of the measurement is, what factors influence its uncertainty and repeatability and what can be done to achieve a level of those parameters that allows the measurement to be considered reliable.

2. Literature analysis

The standard used to determine position and orientation of the probe tip for robots and articulated arms is the Denavit-Hartenberg (D-H) notation, which takes into account the geometry and angular relationships of the individual joints [3,4].In articulated measuring arms or robots, the determination of individual joint angles is based on measurements from encoders placed directly on the axis of rotation. This ensures a very high accuracy of measurement and limits the influence of the sensor mounting on the angle measurement. Factors affecting the uncertainty of measurement are the geometry of each arm component and the connections between the individual components, particularly with regard to the six rotary joints. The new measuring arm solution analyzed in this paper uses accelerometers [5] to determine the joint angles. As this is a completely new approach, it requires the determination of an accuracy and repeatability parameters for such constructed measuring arm. A characteristic feature for accelerometric sensors is the invariability of the accelerometer readings at static measurement for rotation of the accelerometer around the vertical. The consequence of this fact is the inability to measure at the vertical (with respect to gravity direction) axis of rotation of the joint, which limits their industrial applications.

The practice often used by manufacturers of measuring machines and robots of stating the accuracy of a realized measurement as the accuracy of the measuring device leads to misinterpretation of this information [2]. In case of robots, the quoted accuracy and repeatability refer to reaching a position by the tip of the kinematic structure and in case of measuring arms the quoted accuracy and repeatability refer to a

* Corresponding author.
E-mail address: agnieszka.kobierska@p.lodz.pl (A. Kobierska).

https://doi.org/10.1016/j.measurement.2022.111960
Received 16 December 2021; Received in revised form 13 September 2022; Accepted 14 September 2022
Available online 26 September 2022

parameter used by the end user.

The accuracy of the measurements is limited primarily by the feasibility of the construction of the components of the measuring equipment and the type of measurement sensors used. Additionally, in the case of single measurements involving measuring arms, it is not possible to use statistical methods of evaluation of uncertainty of measurement (standard uncertainty type A [6,7]) because of their experimental character [8].

The literature related to repeatability and accuracy measurements for robots and articulated measuring arms mainly focuses on the study of measurement accuracy and methods for its determination [9] and their calibration [10,11]. In [12], the three-dimensional position measurement uncertainty space for an articulated arm measuring machine was determined based on neural network learning with feature point position determination for a normalized cone. The use of a virtual model of the articulated arm to determine the measurement uncertainty space for both position and orientation of the measuring tip is described in [13–15]. The use of the virtual model allowed for a graphical representation of the correlation relationships between the error components, this solution can be applied to non-linear models and additionally through the use of neural networks or Monte Carlo simulations [15–18] takes into account (standard uncertainty type B) the probability density function of quantities that are not determined by statistical processing from measurements (standard uncertainty type A). It is shown in [19], based on D-H and Jacobian notation of the arm, that the measurement uncertainties of the arm design parameters (a_i, d_i) and the distance of the first axis from the base system directly affect the total measurement uncertainty as a constant value, while the measurement uncertainties of the trigonometric function parameters for the angles (α_i and θ_i) affect not only by the joint design parameters but also by the arm alignment. The angle sensors used, which have a large influence on the accuracy of α_i and θ_i, must be very precise, but it is not stated what the minimum accuracy value of these measurement elements is. In [20], a method is shown to integrate the uncertainty of the measurements of the arm design parameters together with the position assumed by the arm in the working area and its effect on the total measurement uncertainty of the arm in the form of D-H notation with the rules described in the Guide to the Expression of Uncertainty in Measurement (GUM) [7,21]. The working areas of the measuring arm where the lowest standard deviation of the measurement is achieved are presented. In [22], it was proposed to reduce the total uncertainty of a measurement performed with an articulated measuring arm by applying a multi-position measurement model using D-H notation and the Levenberg-Marquardt (LM) algorithm to determine the arm calibration. A single-position measurement model was compared to a multi-position measurement model in the arm working space, showing a 40 % improvement in the measurement uncertainty score in favor of the multi-position measurement model for arm calibration.

However, all of the measurement uncertainty studies discussed here have involved robots and arms using precision angular position sensors (encoders), with no constraints on their setup or the cost of the sensors themselves. The cost of the sensors used in robots and arms is significantly out of line with the feasibility of using them in disposable arms for medical applications, which is a reason to look for a solution that meets these criteria. Attempts are being made to develop new sensors using such physical phenomena related to capacitance [23], magnetoresistance [24–26] and optical ones [27]to provide an alternative to encoders. Often, however, these solutions prove not to meet the size requirements, do not take into account the specifics of operation in medical environments, and are not available as devices for commercial applications due to their experimental nature. The use of accelerometers for position measurements [28], in contrast to their basic operation in inertial navigation [29], is an innovative application that requires testing.

3. Construction and principle of arm operation

3.1. Construction

The NaviFast 6D device is a short-reach measuring arm used to measure linear and angular positions in all degrees of freedom. This arm was developed for surgeons to measure the correct fixation of hip prostheses during hip endoprosthetics surgery (Fig. 1). Due to the environment in which the arm works - the possibility of blood contamination or flooding, as well as the requirements of relatively low production costs, it was not possible to use classical measuring systems. An innovative solution was decided upon, in which the measurement is performed using MEMS sensors aimed to measure accelerations.

However, in the presented application it is a static measurement - only the direction of gravitational acceleration is measured. The NaviFast 6D device consists of 7 segments (Fig. 2) connected by rotational joints. In each segment, there is a triaxial MEMS accelerometer connected to the computational and control system located on segment 3.

Segments 1 and 7 are attached to the femur bone and hip plate, respectively, using special quick disconnects.

The proper kinematics of the arm is the key issue to this solution - accelerometers are able to measure the angle of rotation at the arm joint provided that the joint axis is not vertical. This paper will analyze the impact of the proposed innovative measurement method on the repeatability of the measurement and will determine the allowable limits of variation of individual configuration parameters. Chapter 3.2 will present classical formulas for determining position based on articulated angles, and Chapter 3.3 will present formulas for determining articulated angles based on accelerometer readings.

Chapter 4 will present a methodology for determining measurement repeatability based on accelerometer uncertainty and the uncertainty propagation method, along with a presentation of the computational results of this analysis, and Chapter 5 will present experimental studies to determine both accelerometer uncertainty and measurement arm repeatability, along with a comparison of these results with theoretical predictions.

3.2. Position determination based on D-H matrix and theta angles

The coordinate systems Ox_i, z_i, $i = 0\ldots6$ according to Denavit-Hartenberg notation, shown in Fig. 2, were defined on each of the 7 segments of the measuring arm. For these coordinate systems, the individual D-H parameters shown in Table 1 were determined.

Moreover, additional coordinate systems $Ox_By_Bz_B$, $Ox_Ey_Ez_E$ can be defined on segment 0 (treated as the base) and segment 6 (treated as the effector), directly related to the characteristic points relative to which the measurement takes place. In the further part of the article, we will treat the determination of the position and orientation of the last segment in relation to the first segment, recorded in the form of a homogeneous matrix A^E, as a measurement for such a defined measuring arm:

$$A_B^E = A_B^0 A_0^1 A_1^2 A_2^3 A_3^4 A_4^5 A_5^6 A_6^E \tag{1}$$

However, since for the issues of measurement repeatability and for the demonstration of the key dependencies allowing the calculation of this repeatability, the definition of specific systems is not very important and the matrices A_B^0, A_6^E are constant, in the following it is assumed that the systems $Ox_By_B\ z_B$, $Ox_Ey_Ez_E$ are equivalent to the systems $Ox_0y_0\ z_0$, $Ox_6y_6z_6$, respectively, and the determined homogeneous matrix has the form.

$$A = A_0^6 = A_0^1 A_1^2 A_2^3 A_3^4 A_4^5 A_5^6 \tag{1*}$$

Fig. 1. Appearance of the measuring arm attached to the femur and hip bone model.

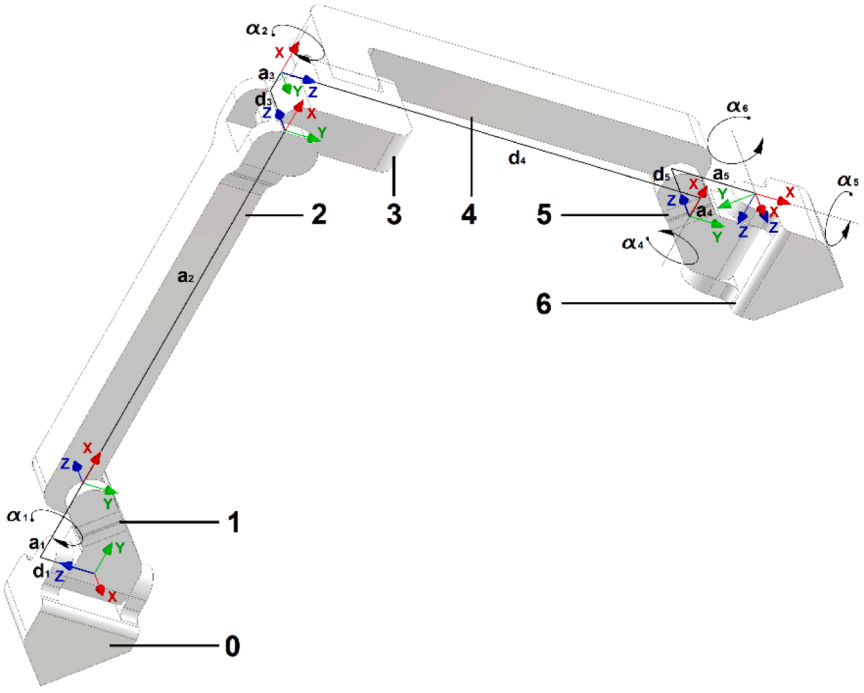

Fig. 2. D-H coordinate systems associated with individual joints and links.

Table 1
NaviFast6D Arm D-H Parameters.

Joint number	θ_i	d_i [mm]	a_i [mm]	α_i [°]
1	θ_1	13	20	−90
2	θ_2	0	95	0
3	θ_3	15	5	−90
4	θ_4	100	−5	90
5	θ_5	18	20	−90
6	θ_6	0	0	45

$$A_{i-1}^{i} = \begin{bmatrix} \cos\theta_i & -\sin\theta_i\cos\alpha_i & \sin\theta_i\sin\alpha_i & a_i\cos\theta_i \\ \sin\theta_i & \cos\theta_i\cos\alpha_i & -\cos\theta_i\sin\alpha_i & a_i\sin\theta_i \\ 0 & \sin\alpha_i & \cos\alpha_i & d_i \\ 0 & 0 & 0 & 1 \end{bmatrix} \quad (2)$$

According to [18], in a homogeneous transformation matrix, we can extract the elements responsible for the displacement (d) and the

orientation of the effector (R):

$$\boldsymbol{A} = \begin{bmatrix} \boldsymbol{R}_0^6 & \boldsymbol{d}_0^6 \\ 0 & 1 \end{bmatrix} \tag{3}$$

Another way to describe orientation is to determine the *roll, pitch*, and *yaw* angles based on the relationship:

$$R_{roll(\gamma)-pitch(\beta)-yaw(\alpha)} = \begin{bmatrix} \cos(\beta)\cos(\gamma) & \sin(\alpha)\sin(\beta)\cos(\gamma) - \cos(\alpha)\sin(\gamma) & \cos(\alpha)\sin(\beta)\cos(\gamma) + \sin(\alpha)\sin(\gamma) \\ \cos(\beta)\sin(\gamma) & \sin(\alpha)\sin(\beta)\sin(\gamma) + \cos(\alpha)\sin(\gamma) & \cos(\alpha)\sin(\beta)\sin(\gamma) - \sin(\alpha)\sin(\gamma) \\ -\sin(\beta) & \sin(\alpha)\cos(\beta) & \cos(\alpha)\cos(\beta) \end{bmatrix} = = \boldsymbol{R}_0^6 \tag{4}$$

In this way, we determine the vector L in the form:

$$\boldsymbol{L} = \left[L_p, O_{\gamma,\beta,\alpha}\right] = \left[L_x, L_y, L_z, roll(\gamma), pitch(\beta), yaw(\alpha)\right]^T \tag{5}$$

contains the displacement vector $\boldsymbol{L_p} = \left(\boldsymbol{d}_0^6\right)^T$ and angular data $O_{\gamma,\beta,\alpha}$ regarding effector orientation in relation to the base.

3.3. Theta determination based on a single measurement

The parameters a_i, d_i, α_i are defined for a given manipulator by its design. In the following part, it will be assumed that they are invariant during the use of the arm and thus do not affect repeatability. For computational purposes, their value will be assumed to be consistent with theoretical parameters. The determination of each angle $\theta_1 \div \theta_6$ is determined by measurements from the accelerometers. Each accelerometer measures the value of acceleration in three directions:

$$Y_i = \left[a_{ccx_i} \quad a_{ccy_i} \quad a_{ccz_i}\right]^T \tag{6}$$

To describe the gravitational acceleration vector E_i in the coordinate system according to the D-H notation for each segment and measuring arm, we can write:

$$E_i = \begin{bmatrix} e_{x_i} \\ e_{y_i} \\ e_{z_i} \end{bmatrix} = \omega_i * \begin{bmatrix} Y_i \\ 1 \end{bmatrix} \tag{7}$$

where ω_i is a sensor calibration matrix of dimension 4×3. The process of calibrating the arm and determining the calibration matrices ω_i is described in [6]. The calibration matrix is constructed so that it corrects for the static error of the accelerometers, proportionality factors, scales the measurement so that the nominal length of the vector E_i is equal to 1, and includes a multiplication by the rotation matrix so that the individual components are expressed in terms of the D-H system of the segment. The E_i vectors determined this way for all accelerometers will be referred to in the remainder of this paper as the output vector or measurement vector:

$$E = [E_0; E_1; E_2; E_3; E_4; E_5; E_6]_{(21\times1)} \tag{8}$$

For two gravitational acceleration vectors E_i and E_{i-1} of adjacent segments of the measuring arm, it is known that:

$$E_{i-1} = \boldsymbol{R}_{i-1}^i * E_i \tag{9}$$

where matrix $\boldsymbol{R}_{i-1}^i$ is part of a homogeneous matrix (2):

$$\boldsymbol{R}_{i-1}^i = \begin{bmatrix} cos\theta_i & -sin\theta_i cos\alpha_i & sin\theta_i ssin\alpha_i \\ sin\theta_i & cos\theta_i cos\alpha_i & -cos\theta_i sin\alpha_i \\ 0 & sin\alpha_i & cos\alpha_i \end{bmatrix} \tag{10}$$

Transforming the above equations we obtain:

$$\begin{bmatrix} e_{x_{i-1}} \\ e_{y_{i-1}} \\ e_{z_{i-1}} \end{bmatrix} = \begin{bmatrix} cos\theta_i & -sin\theta_i cos\alpha_i & sin\theta_i sin\alpha_i \\ sin\theta_i & cos\theta_i cos\alpha_i & -cos\theta_i sin\alpha_i \\ 0 & sin\alpha_i & cos\alpha_i \end{bmatrix} \begin{bmatrix} e_{x_i} \\ e_{y_i} \\ e_{z_i} \end{bmatrix} \tag{11}$$

i.e.

$$\begin{cases} e_{x_{i-1}} = cos\theta_i e_{x_i} - sin\theta_i cos\alpha_i e_{y_i} + sin\theta_i sin\alpha_i e_{z_i} \\ e_{y_{i-1}} = sin\theta_i e_{x_i} + cos\theta_i cos\alpha_i e_{y_i} - cos\theta_i sin\alpha_i e_{z_i} \end{cases} \tag{12}$$

$$\begin{cases} e_{x_{i-1}} = sin\theta_i(-cos\alpha_i e_{y_i} + sin\alpha_i e_{z_i}) + cos\theta_i e_{x_i} \\ e_{y_{i-1}} = sin\theta_i e_{x_i} + cos\theta_i(cos\alpha_i e_{y_i} - sin\alpha_i e_{z_i}) \end{cases} \tag{13}$$

In the notation for solving a system of equations by the determinant method with unknowns sin, cos θ_i:

$$\begin{cases} sin\theta_i(-cos\alpha_i e_{y_i} + sin\alpha_i e_{z_i}) + cos\theta_i e_{x_i} = e_{x_{i-1}} \\ sin\theta_i e_{x_i} + cos\theta_i(cos\alpha_i e_{y_i} - sin\alpha_i e_{z_i}) = e_{y_{i-1}} \end{cases} \tag{14}$$

we obtain:

$$\sin\theta_i = \frac{W_{sin\theta_i}}{W} \tag{15}$$

$$\cos\theta_i = \frac{W_{cos\theta_i}}{W} \tag{16}$$

where

$$W = e_{x_i}^2 + \left(-cos\alpha_i e_{y_i} + sin\alpha_i e_{z_i}\right)^2 = e_{x_{i-1}}^2 + e_{y_{i-1}}^2 \tag{17}$$

$$W_{sin\theta_i} = e_{y_{i-1}} e_{x_i} + e_{x_{i-1}}\left(-cos\alpha_i e_{y_i} + sin\alpha_i e_{z_i}\right) \tag{18}$$

$$W_{cos\theta_i} = e_{x_{i-1}} e_{x_i} - e_{y_{i-1}}\left(-cos\alpha_i e_{y_i} + sin\alpha_i e_{z_i}\right) \tag{19}$$

This system of equations is solvable under the condition that $W \neq 0$. A more detailed analysis shows that this condition is the same as when the axis z_{i-1} is deviated from the vertical. We determine the angles θ_i from the *atan2* function of the form:

$$\theta_i = atan2(\sin\theta_i, \cos\theta_i) = atan2\left(W_{sin\theta_i}, W_{cos\theta_i}\right) \tag{20}$$

Assuming that θ_i is from the range $\left(-\frac{\pi}{2}, \frac{\pi}{2}\right)$, it can be written:

$$\theta_i = \text{atan}\left(\frac{e_{y_{i-1}} e_{x_i} + e_{x_{i-1}}\left(-cos\alpha_i e_{y_i} + sin\alpha_i e_{z_i}\right)}{e_{x_{i-1}} e_{x_i} - e_{y_{i-1}}\left(-cos\alpha_i e_{y_i} + sin\alpha_i e_{z_i}\right)}\right). \tag{20*}$$

From the above formulas, it is clear that the procedure for determining the individual angles θ_i depends on the components of the gravitational acceleration vectors E_i (in the form e_{xi}, e_{yi}, e_{zi}) and E_{i-1} (in the form e_{xi-1}, e_{yi-1}) and the angles αi between the z_{i-1} and z_i axes

measured around the x_i axis of particular segments. Relationship (6) indicates that the input values of the components of the gravitational acceleration vectors and the angle α_i of the individual segments are correlated, which will affect the calculation of the composite standard uncertainty of the measurement of the angles θ_i. In order to correctly determine the uncertainty in the following relationships, it is important to note that the values of E_i depend on the orientation of the entire arm with respect to the direction of the gravity vector. In order to determine these relationships, the coordinate system $Ox_Gy_Gz_G$ was additionally defined to define the vertical direction. The z_G axis of the gravity system is up and the x_G axis of the gravity system coincides with the projection of the z_0 axis (the axis of rotation of the first joint) on the horizontal. The position of the arm was defined by the position of the segment 0 with respect to the gravitational system G. This definition cannot be determined in an arbitrary way due to the possibility of oddness. The two angles β_y and β_z of rotation of system 0 with respect to the gravitational system G (with z-axis pointing vertically upward) were defined as follows: β_y - angle between z_G and z_0 (deviation of the z_0 axis from vertical) - always positive; β_z - angle between y_G and y_0 (rotation of the base segment about the axis of joint 1). This can be represented by the following relationships:

$$R_G^o(\beta_y, \beta_z) * \mathrm{E}_o = \begin{bmatrix} 0 \\ 0 \\ 1 \end{bmatrix} \tag{21}$$

$$R_G^o = R_{y,\beta_y} R_{z,\beta_z} = \begin{bmatrix} cos\beta_y cos\beta_z & -cos\beta_y sin\beta_z & sin\beta_y \\ sin\beta_z & cos\beta_z & 0 \\ -sin\beta_y cos\beta_z & sin\beta_y sin\beta_z & cos\beta_y \end{bmatrix} \tag{22}$$

i.e.

$$E_0 = \begin{bmatrix} -sin\beta_y cos\beta_z & sin\beta_y sin\beta_z & cos\beta_y \end{bmatrix}^T \tag{23}$$

Based on these records, it can be seen that the full vector of configuration variables describing the static position of the measurement arm is eight-element:

$$X = \left[\theta_1, \theta_2, \theta_3, \theta_4, \theta_5, \theta_6, \beta_y, \beta_z\right] \tag{24}$$

and is extended relative to the classical six-element state vector by the elements β_y, β_z specifying the orientation of the arm base relative to the vertical. On the basis of such a defined vector of configuration variables, both the homogeneous matrix (1) and the output variables of the measurement system can be determined:

$$\begin{aligned} E_i &= R_i^G * [0,0,1]^T = \left(R_G^i\right)^{-1} * [0,0,1]^T = \\ &= \left(R_G^i\right)^T * [0,0,1]^T = \left(R_G^0 R_0^1 \cdots R_{i-1}^i\right)^T * [0,0,1]^T = \\ &= \left(R_G^0 \bigcup_{j=1}^{i} R_{j-1}^j\right)^T * [0,0,1]^T \end{aligned} \tag{25}$$

3.4. Novelty of the paper

It is easy to see that when the system of Eqs. (14) is unsolvable, i.e., $W = 0$, it is equivalent to the conditions $e_{x_i} = 0$ and $-cos\alpha_i e_{y_i} + sin\alpha_i e_{z_i} = 0$, which in turn is equivalent to.

$e_{x_{i-1}} = 0 i e_{y_{i-1}} = 0$, meaning that the z_{i-1} axis is vertical. This is the relationship that should have been expected and is the primary limitation of this method of measuring angular position - by measuring the direction of the gravity field. Thus, it is to be expected that for arm settings with either joint axis vertical, the uncertainty in the measurement of position $u(L)$ and orientation $u(RPY)$ will grow in the limit to infinity (for the situation where we linearize the uncertainty propagation model). Subsequent chapters and the entire article will lead to the derivation of relationships for changes the repeatability - one of the parameters connected to the measurement uncertainty $u(L)$, $u(RPY)$ when approaching the vertical with either axis of rotation, and further to determine the range of applicability of the measuring arm. Since no such method of measuring the rotation angle has been used in any of the devices built so far in the world, so no analysis of its repeatability has been carried out either. This analysis will additionally allow for the precise definition of the method of attaching the NaviFast6D measuring arm to the patient. Since the application of the arm is related to the task of reconstructing the state of the hip joint prior to surgery, so in this paper we will only limit ourselves to the repeatability analysis, and the variables denoting the measurement uncertainty $u(L)$, $u(RPY)$ will be discussed in further research.

4. Theoretical determination of measurement repeatability as a function of the measurement point position in the measurement space with eight degrees of freedom

4.1. Analysis of factors affecting repeatability and methodology for determining repeatability

There are many parameters that describe the quality of a measurement using a measuring arm. In this paper, we will mainly be concerned with the repeatability of the measurement. In Chapter 3.3, the relationship between the angles θ_i and the components of the gravitational acceleration vectors E_i was shown. The main factor affecting the repeatability of the described measurement arm is the repeatability of the applied measurement element (measurement noise), in the described case of accelerometers. An additional source of noise may be external vibrations reflected in the accelerometers reading. Additionally, variable deflection of individual device segments resulting from friction forces in the joints may have an impact on the measurement repeatability. It was assumed that the mechanical structure of the device has no backlash and its influence on repeatability of measurement is negligible.

4.2. Determination of the equations for measurement repeatability

The vector L described in Chapter 3.2 is the function $L = f(\alpha_i, a_i, d_i, \theta_i)$ for i = 1.0.6, where α_i, a_i, d_i are fixed values resulting from the arm design entered into the D-H matrix, while the angles θ_i are calculated from measurements using accelerometers.

Repeatability for manipulators and robots is defined as the degree of agreement between the results of successive measurements of the same measured value, performed under the same measurement conditions and with the same device [30,31]. For manipulators, position repeatability consists of position repeatability and tip orientation repeatability (TCP point) of the motorized arm.

Position repeatability is defined as the radius of a sphere (RP), whose center is also the center of the set of points of its workspace (Fig. 3):

$$RP_l = \bar{l} \pm 3S_L \tag{26}$$

where the standard deviation of the position S_L was determined by the formula:

$$S_L = \sqrt{\frac{\sum_{j=1}^{n} \left(l_j - \bar{l}\right)^2}{(n-1)}} \tag{26a}$$

$$\bar{l} = \frac{1}{n} \sum_{j=1}^{n} l_j \tag{26b}$$

$$l_j = \sqrt{\left(x_j - \bar{x}\right)^2 + \left(y_j - \bar{y}\right)^2 + \left(z_j - \bar{z}\right)^2} \tag{26c}$$

For - $\bar{x}$, $\bar{y}$ and $\bar{z}$ - as the average coordinates of the workspace points obtained by obtaining the set position n times; x_j, y_j and z_j - the coordinates of the actual position obtained with the j-th movement to the

set position.

Orientation repeatability is defined as the spread of angles ± 3Sγ, ±3Sβ, ±3Sα from the mean values *roll* - $\bar{\gamma}$, *pitch* - $\bar{\beta}$, *yaw* - $\bar{\alpha}$, where Sγ, Sβ, Sα are the normalized deviations of the real orientation distribution:

$$RP\gamma = \pm 3S\gamma = \pm 3\sqrt{\frac{\sum_{j=1}^{n}\left(\gamma_j - \bar{\gamma}\right)^2}{(n-1)}} \tag{27}$$

$$RP\beta = \pm 3S\beta = \pm 3\sqrt{\frac{\sum_{j=1}^{n}\left(\beta_j - \bar{\beta}\right)^2}{(n-1)}} \tag{28}$$

$$RP\alpha = \pm 3S\alpha = \pm 3\sqrt{\frac{\sum_{j=1}^{n}\left(\alpha_j - \bar{\alpha}\right)^2}{(n-1)}} \tag{29}$$

where: $\bar{\gamma}$, $\bar{\beta}$ and $\bar{\alpha}$– mean value of orientation angles, γ_j, β_j and α_j – real orientation angles obtained at the j-th repetition.

For the presented arm, we have 6 parameters θ_i describing the angular position of the arm joints. According to the uncertainty propagation law [32], the covariance matrix $Cov(L)$ of measurement result L for correlated variables has the form:

$$Cov(L) = \sum_{i=1}^{6}\left(\frac{\partial f}{\partial \theta}\right)^2 S^2(\theta_i) + 2\sum_{i=1}^{5}\sum_{j=i+1}^{6}\frac{\partial f}{\partial \theta_i} * \frac{\partial f}{\partial \theta_j} * Cov(\theta_i, \theta_j) \tag{30}$$

components of the gravitational field is a composite of the standard deviation of the accelerometer readings. To determine the variances and covariances matrix in the determination of the angles θ_i, as defined by equation (32), the following relationship can be used:

$$Cov(\theta) = J_{\theta/E} * Cov(E) * J_{\theta/E}^T \tag{33}$$

where the matrix Cov(E) is a diagonal matrix containing on its diagonal the variances of the individual variables determined by methods A and B. On the other hand, the Jacobian of the derivatives $J_{\theta/E}$ is calculated from equation (6). The equations of partial derivatives of the function θ_i after the parameters of the vector E take the form:

$$\frac{\partial \theta_i}{\partial e_{x_{i-1}}} = \frac{-e_{y_{i-1}}}{e_{x_{i-1}}^2 + e_{y_{i-1}}^2}; \quad \frac{\partial \theta_i}{\partial e_{y_{i-1}}} = \frac{e_{x_{i-1}}}{e_{x_{i-1}}^2 + e_{y_{i-1}}^2}; \quad \frac{\partial \theta_i}{\partial e_{z_{i-1}}} = 0; \tag{34a,b,c}$$

$$\frac{\partial \theta_i}{\partial e_{x_i}} = \frac{e_{y_i} cos\alpha_i - e_{z_i} sin\alpha_i}{e_{y_i}^2 cos\alpha_i^2 + e_{z_i}^2 sin\alpha_i^2 + e_{x_i}^2 - 2e_{y_i} e_{z_i} cos\alpha_i sin\alpha_i}; \tag{34d}$$

$$\frac{\partial \theta_i}{\partial e_{y_i}} = \frac{-e_{x_i} cos\alpha_i}{e_{y_i}^2 cos\alpha_i^2 + e_{z_i}^2 sin\alpha_i^2 + e_{x_i}^2 - 2e_{y_i} e_{z_i} cos\alpha_i sin\alpha_i}; \tag{34e}$$

$$\frac{\partial \theta_i}{\partial e_{z_i}} = \frac{e_{x_i} sin\alpha_i}{e_{y_i}^2 cos\alpha_i^2 + e_{z_i}^2 sin\alpha_i^2 + e_{x_i}^2 - 2e_{y_i} e_{z_i} cos\alpha_i sin\alpha_i}; \tag{34f}$$

Given the angles ($\theta_{1\div 6}$), we determine the Jacobian of the derivatives $J_{\theta/E}$:

$$J_{\theta/E} = \begin{bmatrix} \frac{\partial\theta_1}{\partial e_{x_0}} & \frac{\partial\theta_1}{\partial e_{y_0}} & 0 & \frac{\partial\theta_1}{\partial e_{x_1}} & \frac{\partial\theta_1}{\partial e_{y_1}} & \frac{\partial\theta_1}{\partial e_{z_1}} & 0 & 0 & 0 & 0 & 0 & 0 & \cdots & 0 & 0 & 0 \\ 0 & 0 & 0 & \frac{\partial\theta_2}{\partial e_{x_1}} & \frac{\partial\theta_2}{\partial e_{y_1}} & 0 & \frac{\partial\theta_2}{\partial e_{x_2}} & \frac{\partial\theta_2}{\partial e_{y_2}} & \frac{\partial\theta_2}{\partial e_{z_2}} & 0 & 0 & 0 & & 0 & 0 & 0 \\ 0 & 0 & 0 & 0 & 0 & 0 & \frac{\partial\theta_3}{\partial e_{x_2}} & \frac{\partial\theta_3}{\partial e_{y_2}} & 0 & \frac{\partial\theta_3}{\partial e_{x_3}} & \frac{\partial\theta_3}{\partial e_{y_3}} & \frac{\partial\theta_3}{\partial e_{z_3}} & & 0 & 0 & 0 \\ 0 & 0 & 0 & 0 & 0 & 0 & 0 & 0 & 0 & \frac{\partial\theta_4}{\partial e_{x_3}} & \frac{\partial\theta_4}{\partial e_{y_3}} & 0 & & \frac{\partial\theta_4}{\partial e_{x_4}} & \frac{\partial\theta_4}{\partial e_{y_4}} & \frac{\partial\theta_4}{\partial e_{z_4}} \\ 0 & 0 & 0 & 0 & 0 & 0 & 0 & 0 & 0 & 0 & 0 & 0 & & \frac{\partial\theta_5}{\partial e_{x_4}} & \frac{\partial\theta_5}{\partial e_{y_4}} & 0 \\ 0 & 0 & 0 & 0 & 0 & 0 & 0 & 0 & 0 & 0 & 0 & 0 & & 0 & 0 & 0 \end{bmatrix}$$

$$\begin{bmatrix} 0 & 0 & 0 & 0 & 0 & 0 & 0 & 0 & 0 \\ 0 & 0 & 0 & 0 & 0 & 0 & 0 & 0 & 0 \\ 0 & 0 & 0 & 0 & 0 & 0 & 0 & 0 & 0 \\ 0 & 0 & 0 & 0 & 0 & 0 & 0 & 0 & 0 \\ \frac{\partial\theta_5}{\partial e_{x_5}} & \frac{\partial\theta_5}{\partial e_{y_5}} & \frac{\partial\theta_5}{\partial e_{z_5}} & 0 & 0 & 0 & 0 & 0 & 0 \\ \frac{\partial\theta_6}{\partial e_{x_5}} & \frac{\partial\theta_6}{\partial e_{y_5}} & 0 & \frac{\partial\theta_6}{\partial e_{x_6}} & \frac{\partial\theta_6}{\partial e_{y_6}} & \frac{\partial\theta_6}{\partial e_{z_6}} & 0 & 0 & 0 \end{bmatrix}_{6x21} \tag{35}$$

which is equivalent to the notation:

$$Cov(L) = J_{\frac{L}{\theta}} Cov(\theta) J_{\frac{L}{\theta}}^T \tag{31}$$

Jacobian J_L is calculated from the equations of simple kinematics of the manipulator as the derivative of the scalar function of the Jacobian matrix according to [4]. The variances and covariances of the individual joint variables can be written in matrix form:

$$Cov(\theta) = \begin{bmatrix} S^2(\theta_1) & \cdots & cov(\theta_1\theta_6) \\ \vdots & \ddots & \vdots \\ cov(\theta_6\theta_1) & \cdots & S^2(\theta_6) \end{bmatrix}_{6x6} \tag{32}$$

We calculate the parameters θ_i by measuring the direction of the gravitational field from 7 accelerometers as a vector of input variables E according to equation (8). Each accelerometer measures in three mutually perpendicular directions, resulting in a total of 21 possible variables affecting the measurement standard deviation of the joint variables θ_i. The measurement standard deviation of the vector E

The matrix Cov(θ) can be used to determine the uncertainty of the transform T_0^6 from system 6 to 0, and then to determine the standard deviation of determination of the displacement vector.

$\boldsymbol{L} = \left[L_x, L_y, L_z, yaw(\alpha), pitch(\beta), roll(\gamma)\right]$. The designated Jacobian $J_{\theta/E}$ can then be used to calculate the covariance matrix of measurement $Cov(L)$.

$$Cov(L) = J_{L/\theta} J_{\theta/E} Cov(E) J_{\theta/E}^T J_{L/\theta}^T \tag{36}$$

The resulting value of the standard deviation for the position expressed as:

$$S_L = \sqrt{Cov(L)_{(1,1)} + Cov(L)_{(2,2)} + Cov(L)_{(3,3)}} \tag{37}$$

and standard deviation for orientation:

$$S_{roll} = \sqrt{Cov(L)_{(4,4)}}; \; S_{pitch} = \sqrt{CCov(L)_{(5,5)}}; \; S_{yaw} = \sqrt{Cov(L)_{(6,6)}}$$

$$S_{RPY} = \sqrt{Cov(L)_{(4,4)} + Cov(L)_{(5,5)} + Cov(L)_{(6,6)}} \tag{38}$$

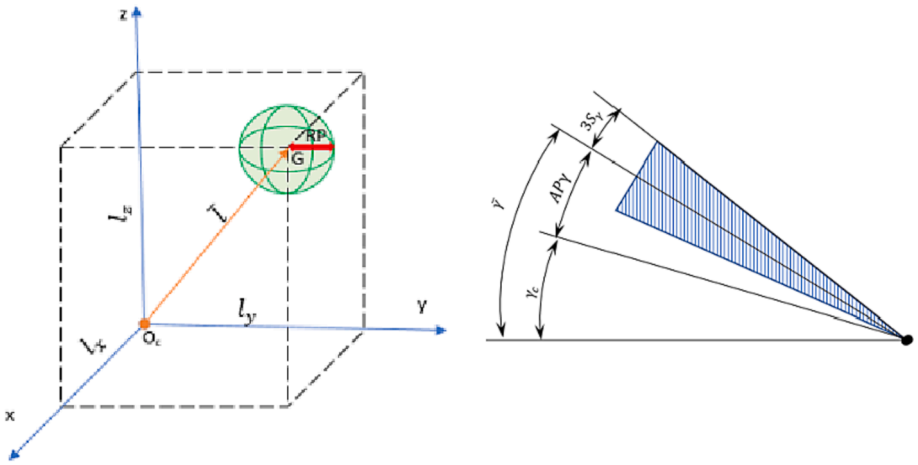

Fig. 3. Repeatability of RP position and orientation RPγ=±3Sγ, where $AP\gamma = (\bar{\gamma} - \gamma c)$ - accuracy of angle γ orientation, determined according to [30].

were used to calculate position repeatability and orientation repeatability according to the formulas (26), (27), (28) and (29).

Since the standard deviation S_L and S_{RPY} have different measures (mm and radians) it was decided to introduce an additional parameter combining all the uncertainty components. This parameter can be defined as the average standard deviation of determining the position of the effector characteristic point for an assumed distance Δ of this point from the center of the coordinate system of the last arm segment.

$$S_{LRPY} = \sqrt{S_L^2 + (\Delta * S_{RPY})^2} = \sqrt{Cov(L)_{(1,1)} + Cov(L)_{(2,2)} + Cov(L)_{(3,3)} + \Delta^2\left(Cov(L)_{(4,4)} + Cov(L)_{(5,5)} + Cov(L)_{(6,6)}\right)} \tag{39}$$

The value $\Delta = 100\ mm$ was assumed based on the fixing conditions characteristic for the arm application.

4.3. Experimental determination of measurement noise for different types of accelerometers

Testing of measurement noise variation depending on the angular orientation of the sensors in the measurement space and on the type of accelerometer was carried out on a test stand equipped with a plate containing 5 types of accelerometric sensors, 4 of each type. The PCB plate was mounted at the end of the referencing device equipped with two rotary joints connected in series with perpendicular to each other axes a_1 and a_2, where axis a_1 was fixed and oriented horizontally. Rotation around both axes allowed the plate with sensor to be placed at any angle with respect to the gravitational field vector axis.

The test consisted in collecting in 1 s 100 samples of data from each accelerometer for each of its axes, with changing positions of the PCB. The measurement procedure consisted in collecting data for the stationary a_1 axis at successive positions of the a_2 axis in the range from 0 to 340° in 20° steps and then repeating the procedure for the a_1 axis rotated by 20°. Rotation of the a_1 axis was performed in the range from 0° to 180°, which allowed to perform measurements for 180 positions of the plate in total.

Standard deviation values σ_{jk} for one sensor were expressed as the root of the arithmetic mean of the variance of each of the three axes of sensor j aligned to one position k during a single measurement (n = 100 samples).

Table 2
Operating parameters and cost for selected types of accelerometric sensors.

	Range [g]	Resolution [bit]	Price [USD]
ADXL355	2	20	$57,36
LIS3DHH	2,5	16	$9,33
LIS331	2	16	$2,99
KX023	2	16	$2,14
MMA9551	2	16	$2,97
FXLS8471Q	2	14	$4,00

$$\sigma_{jk} = \sqrt{\frac{\frac{\sum_{i=1}^{n}(x_{ijk}-\bar{x}_{jk})^2}{n} + \frac{\sum_{i=1}^{n}(y_{ijk}-\bar{y}_{jk})^2}{n} + \frac{\sum_{i=1}^{n}(z_{ijk}-\bar{z}_{jk})^2}{n}}{3}} \tag{40}$$

where: x_{ijk}, y_{ijk}, z_{ijk} - values of particular indications of OX, OY, OZ axes of accelerometer, $\bar{x}_{jk}, \bar{y}_{jk}, \bar{z}_{jk}$ mean values from n samples.

The value of the standard deviation σ_{jkl} for a given sensor type based on $l = 4$ pieces in all $m = 180$ positions, whose individual standard deviations σ_{jk} were determined by the formula:

$$\sigma_{jkl} = \frac{\sum_{j=1}^{l}\sum_{k=1}^{m}\sigma_{jk}}{lm} \tag{41}$$

where: $l = 4$ - number of sensors of a given type, $m = 180$ – number of positions.

The measurement noise variation results summarized in Table 3 show significant discrepancies between manufacturers' data and actual data.

The values are presented in "standard gravity" units ([g]) and in increments ([Inc.]) of each sensor. The manufacturer's data were calculated based on the "Output noise density" parameter reported in the documentation. Based on the conducted experiments (Table 3) and cost analysis (Table 2), a standard deviation for the FXLS8471Q sensor equal to 0.0008 [g] was assumed for further calculations of measuring arm repeatability. In this specific device NaviFAST 6D the cost is very important that's why the choice of the sensor type based on the best price/quality ratio.

Table 3
Measurement noise variation results depending on angular orientation for selected accelerometer sensor types.

Sensor model	Units	σ_{jklMIN} Minimum standard deviation in a set of sensors	σ_{jklMAX} Maximum standard deviation in a set of sensors	σ_{jkl} Mean standard deviation for a set sensors	The standard deviation σ reported by the manufacturer for f = 100 [Hz]
ADXL355	[Inc.]	17,8	21	19,7	52
LIS3DHH	[Inc.]	6,3	13,3	7,9	5,9
LIS331	[Inc.]	22	25	23	36
KX023	[Inc.]	5,2	7,3	6,2	18
FXLS8471Q	[Inc.]	1,9	5,9	3,2	4
ADXL355	[g]	$6,8 * 10^{-5}$	$8,2 * 10^{-5}$	$7,5 * 10^{-5}$	$2,0 * 10^{-4}$
LIS3DHH	[g]	$4,9 * 10^{-4}$	$1,0 * 10^{-3}$	$6,1 * 10^{-4}$	$4,5 * 10^{-4}$
LIS331	[g]	$1,3 * 10^{-3}$	$1,6 * 10^{-3}$	$1,4 * 10^{-3}$	$2,2 * 10^{-3}$
KX023	[g]	$3,2 * 10^{-4}$	$4,5 * 10^{-4}$	$3,8 * 10^{-4}$	$1,1 * 10^{-3}$
FXLS8471Q	[g]	$4,6 * 10^{-4}$	$1,4 * 10^{-3}$	$8,0 * 10^{-4}$	$9,9 * 10^{-4}$

Table 4
Values of angles β_y and β_z for which vertical alignment of arm joint axes is possible.

No. of vertically aligned axis	β_y [°]	β_z [°]	β_y [°]	β_z [°]
1	0	any	180	any
2	90	150	90	−30
3	90	150	90	−30
4	165	60	15	−120
5	98,54	−64,07	81,46	115,92
6	82,46	−152,93	97,53	27,07

5. Presentation of experimental measurement of repeatability and comparison with simulation results

The algorithm presented above was used to determine two relationships necessary for the proper software of the measuring arm. The first is to determine the minimum number of repetitions of measurements so that the average repeatability of the RP_1 position measurement is within the assumed range of values (0,1 ÷ 0,2 mm), which is also directly related to the time allocated for the measurement and allows for determining the minimum time of the procedure. Based on the algorithm, it is possible to calculate the repeatability value of a single measurement. If we treat as a measurement the average of a series of n readings for a fixed measurement arm setting, then the deviation of the average will be expressed by the formula:

$$S_{\bar{L}} = \frac{S_L}{\sqrt{n}} \tag{42}$$

On this basis, if we know what is the repeatability of a single measurement S_L for a given configuration and we have an assumed repeatability of an average measurement $S_{\bar{L}}$ then we can determine the number of repetitions of a measurement to achieve it.

$$n = \left(\frac{S_L}{S_{\bar{L}}}\right)^2 \tag{43}$$

To achieve the position measurement repeatability at this level, it is required that the average standard deviation $S_{\bar{L}}$ does not exceed 0,05 mm. The second parameter determined by the formulae is the permissible minimum deviation of the individual axes to the vertical based on an assumed increase in measurement standard deviation. These relationships will be shown in the figures.

5.1. Analytical determination of repeatability of a single measurement

The values of matrix $Cov(L)$ and cumulative standard deviation S_{LRPY} depends on all eight state X variables according to equation (24).

Table 5a
Values of angles βy [°] considered in the simulation.

No.	1	2	3	4	5	6	7	8	9	10
β_y[°]	−1,01	−0,09	0,09	1,01	5	10	14	14,91	15,09	16
No.	**11**	**12**	**13**	**14**	**15**	**16**	**17**	**18**	**19**	**20**
β_y[°]	20	30	40	50	60	64	65	65,4	65,58	66
No.	**21**	**22**	**23**	**24**	**25**	**26**	**27**	**28**	**29**	**30**
β_y[°]	67	70	75	79	80	81,37	81,55	82	83	87
No.	**31**	**32**	**33**	**34**	**35**	**36**	**37**	**38**	**39**	**40**
β_y[°]	88	89,91	90,09	91	93	94	95	97	98,45	98,63
No.	**41**	**42**	**43**	**44**	**45**	**46**	**47**	**48**	**49**	**50**
β_y[°]	99	110	113	114,42	114,59	115	120	130	140	150
No.	**51**	**52**	**53**	**54**	**55**	**56**	**57**	**58**	**59**	
β_y[°]	163	164,91	165,09	167	170	178,99	179,91	180,09	181,01	

Table 5b
Values of angles βz [°] considered in the simulation.

No.	1	2	3	4	5	6	7	8	9	10
β_z[°]	−181,01	−180,01	−179,99	−170	−160	−150	−130	−121	−120,1	−119,9
No.	**11**	**12**	**13**	**14**	**15**	**16**	**17**	**18**	**19**	**20**
β_z[°]	−119	−110	−100	−80	−70	−67	−64,16	−63,98	−62	−50
No.	**21**	**22**	**23**	**24**	**25**	**26**	**27**	**28**	**29**	**30**
β_z[°]	−35	−31	−30,09	−29,91	−29	−15	−6	−5,44	−5,26	−5
No.	**31**	**32**	**33**	**34**	**35**	**36**	**37**	**38**	**39**	**40**
β_z[°]	−1,01	−0,09	0,09	1,01	10	20	30	40	50	60
No.	**41**	**42**	**43**	**44**	**45**	**46**	**47**	**48**	**49**	**50**
β_z[°]	70	80	90	100	110	115	115,84	116,02	117	120
No.	**51**	**52**	**53**	**54**	**55**	**56**	**57**	**58**	**59**	**60**
β_z[°]	130	140	149	149,91	150,1	151	160	170	173	174
No.	**61**	**62**	**63**	**64**	**65**					
β_z[°]	175	178,99	179,91	180,09	181,01					

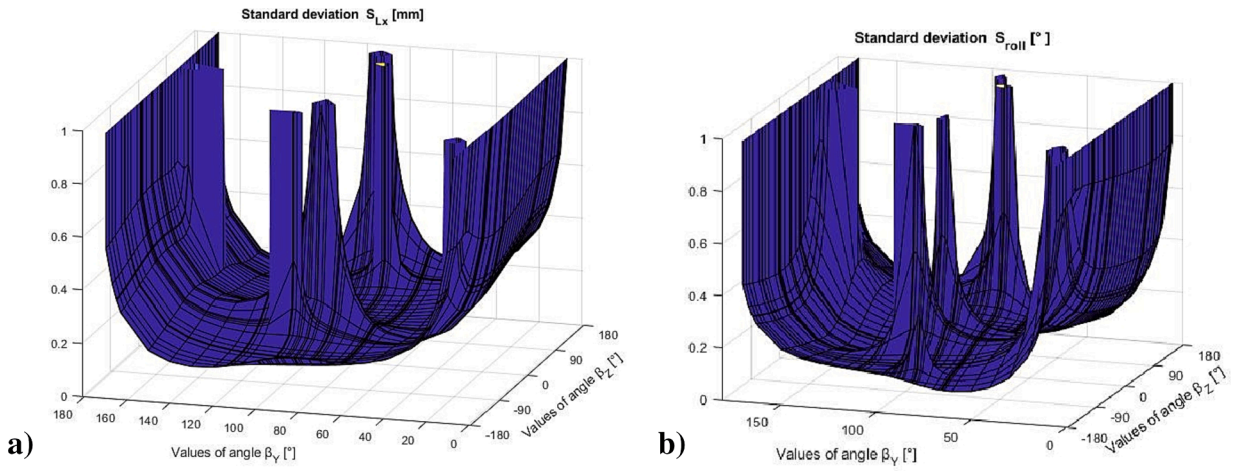

Fig. 4. Calculation results: a) standard deviation Lx b) standard deviation Roll.

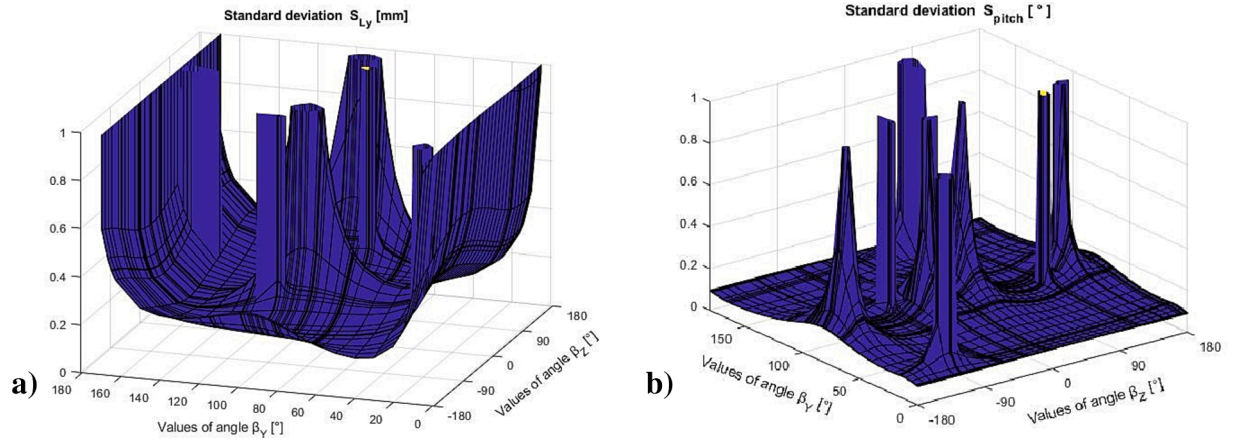

Fig. 5. Calculation results: a) standard deviation Ly b) standard deviation Pitch.

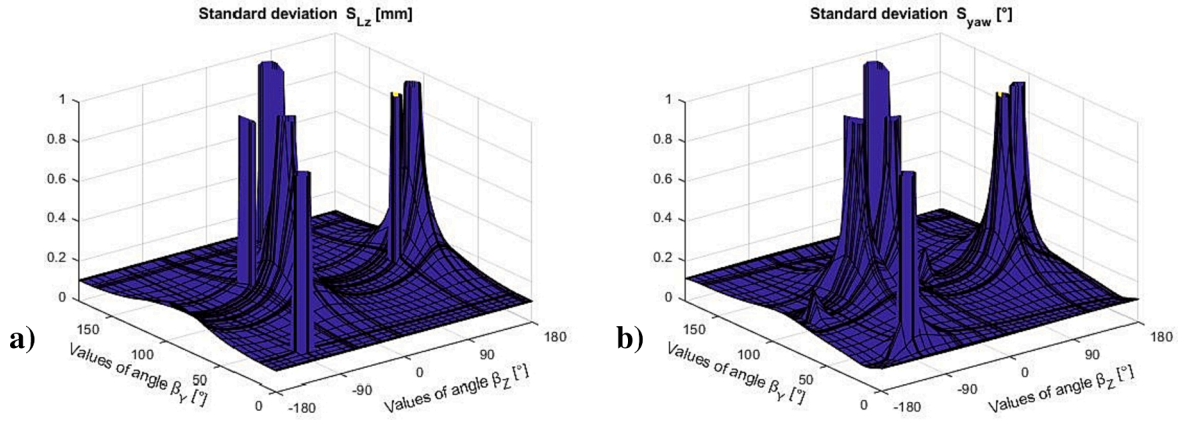

Fig. 6. Calculation results: a) standard deviation Lz b) standard deviation Yaw.

However, it seems pointless to present an analysis of all these dependencies, since the methodology of the procedure will be invariable. It has been decided to carry out the analyses for a constant setting of the measuring arm with the following values of the angles θ_i in the joints expressed in degrees $\theta_{(1\div6)} = [120, 30, -45, -35, 110, 125]$ and for variable values of β_y and β_z as the angles of setting the base of the measuring arm. The selected set of angles on individual joints for the angles $\beta_y = 45°$, $\beta_z = 90°$ represents the middle position of the arm during measurements during surgery.

This setting ensures the correct alignment of the axis of accelerometers (there is no vertical alignment of the axis of the joints - which would exclude the measurement) and allows surgeon to adjust the position of the device to the size of patient (smaller and larger than the adopted average)..

For the assumed interval of the arm base position: β_y from 0° to + 180° and β_z from −180° to + 180°, the values of β_y and β_z were

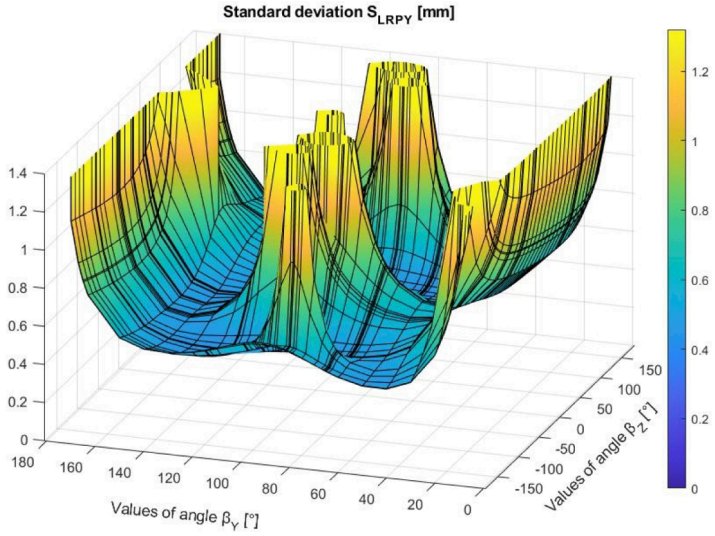

Fig. 7. Calculation results: cumulative standard deviation S_{LRPY} [mm] determined from equation (39).

determined (Table 4) according to formula (25), in which the individual axes of the measuring arm assume the vertical position and therefore high measurement cumulative standard deviation S_{LRPY} are expected. Calculations in Matlab were performed for the values in degrees of angles βy and βz shown in Tables 5a and 5b with an additional density of angle values at the feature points consistent with Table 4.

According to the tests shown in Chapter 4.3, the standard deviation of the accelerometers was assumed to be 0.0008 [g].

The entire space in which the arm repeatability should be considered is eight-dimensional (there are so many independent variables defining the arm's work). The methodology presented in the article shows the method of determining this repeatability in any place in this space. However, since it is not possible to show such dependencies graphically, it was decided to experimentally verify and graphically present these relationships for a selected set of fixed and variable parameters of individual parameters - β_y or β_z, changing them in such a way as to show the key phenomena.

The figures (Figs. 4-6) show the results of the standard deviation calculations for the individual components of the vector L. The results of the calculations for a single measurement at the positions listed in Tables 5a and 5b indicate a significant increase in measurement standard deviation (over 1 mm) at the initial position settings for the arm segment 1 according to Table 4. In other areas, the average standard deviation is $S_L = 0{,}42$ mm for the position according to Equation (37) and $S_{RPY} = 0{,}34°$for the orientation according to Equation (38).

Since the diagrams presented in Figs. 4-6 concern different standard deviation components and have different measures (mm and degrees), the cumulative standard deviation $S_{LRPY}[mm]$ determined from equation (39) is shown in the figures (Fig. 7, Fig. 8). This diagram is presented as a contour plot to clearly show the areas of higher standard deviation coinciding with the singular positions indicated in Table 4.

The diagram (Fig. 8) shows the boundary as an contour lines for the measurement standard deviation where the standard deviation S_{LRPY} does not exceed three times the minimum value of 0,44 mm. At oddness points, the standard deviation S_{LRPY} of the measurement increases in the limit to infinity and for all measurements at positions more than 15° away from the oddness points, the maximum standard deviation S_{LRPY} of the measurement is 1,32 mm. Therefore, it was assumed that the 15° deviation from the oddness points would be the limit at which the oddness could be approached. For the measurement space thus defined, the average standard deviation S_{LRPY} of the measurement is 0,64 mm.

5.2. Construction of test stand

In order to verify the computational method of standard deviation determination using the error propagation method, an experimental study was conducted.

The test stand (Fig. 9) for determining the angular position of the measuring arm in space was constructed in such a way as to make it possible to rotate the arm independently around two axes (φ_1, φ_2) perpendicular to each other and connected in series. The base of the stand was firmly fixed to the ground in such a way that the first axis of rotation of the stand was set to the horizontal position (φ_1). The rotation angles were measured with an accuracy of 0.005° by two 16-bit absolute encoders (3), independently controlling the angular position of each axis. During all measurements, the arm was positioned with the following values of angles θ_i at the joints expressed in degrees $\theta_{(1\div6)} =$ [120, 30, −45, −35, 110, 125].

The verification of the experiment was carried out in two variants:

a) variant I: constant angular position of axis 1 (φ_1) amounting to 295° and variable angular position of axis 2 (φ_2) within the range from 90° to 270° with a step of 5°,
b) variant II: fixed angular position of axis 2 (φ_2) amounting to 180° and variable angular position of axis 1 (φ_1) in the range of −40° to 100° with a step of 5°.

5.3. Results

Experimental studies conducted according to variant II in the central range of angles φ_1 correspond to the positioning of the arm for a typical patient position on the operating table. The experimental study conducted according to variant I correspond to the positioning of the measuring arm from the angular position of the first segment $\beta_y = 15°$ at the characteristic point (4), where the axis 4 approaches the vertical position. On the figure (Fig. 10), there is a characteristic "break", in which the value of the standard deviation for the S_L position goes to infinity. Conducting experiments confirming the repeatability for the entire space of angles β_y and β_z as was done in the theoretical analysis, would be too time-consuming and would not bring new elements to the analysis. Therefore, it was decided to select two sections of the plane β_y, β_z in such a way that they pass through the singular points. In this way, both the correctness of the obtained numerical values of the standard deviation and the phenomenon of loss of repeatability in singular positions were confirmed.

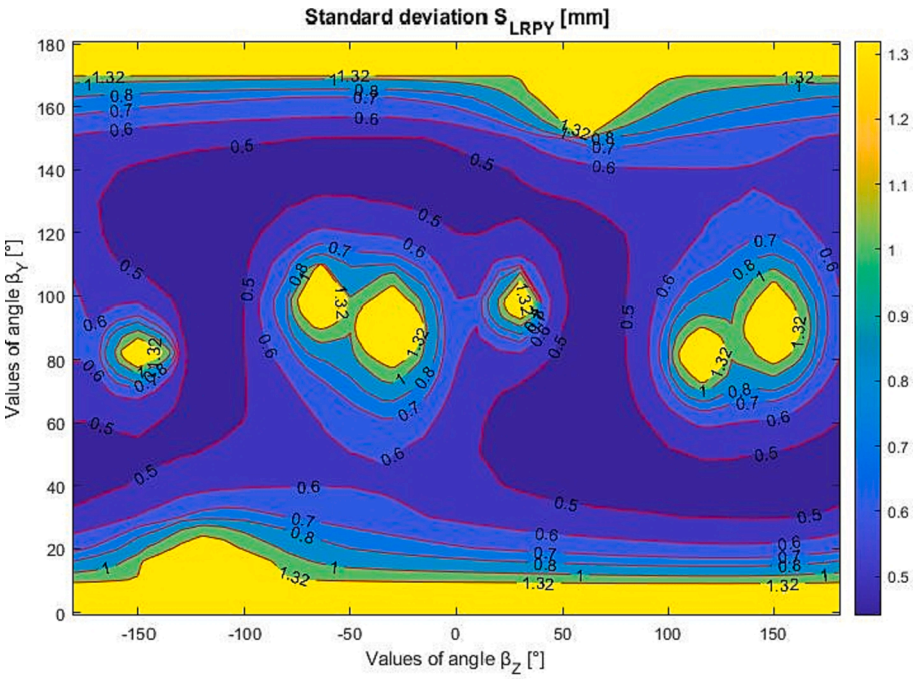

Fig. 8. Calculation results: cumulative standard deviation S_{LRPY} determined from equation (39).

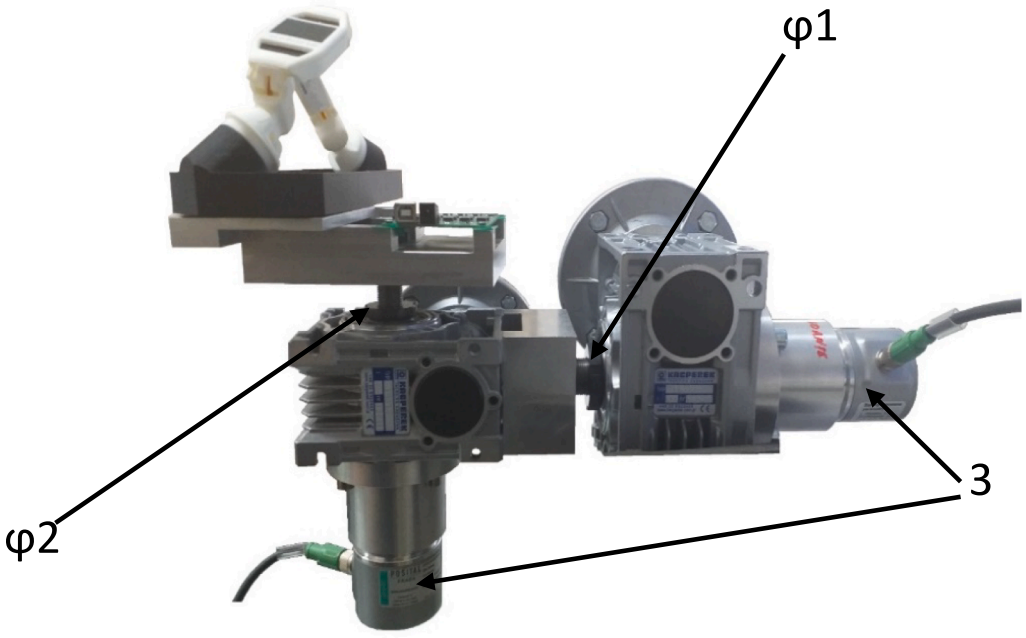

Fig. 9. Test stand for determining the angular position of the measuring arm base.

The experimental results of the standard deviation for the S_L position (Fig. 10, Fig. 11) show a shift of the standard deviation values in comparison with the calculation results while maintaining the trend line. From the medical point of view, the leg evenness should be up to 3 mm. Since the evenness of the legs is influenced by additional errors, such as the repeatability of the doctor's actions, the repeatability of the arm measurement should be at the level of 1 mm at most. The achieved values of standard deviation for the position within the working range of the measuring arm are below the value of 1 mm. The average standard deviation for the tests performed according to the variant I and II of the experiment is for the $S_L = 0.46$ mm. The value of standard deviation obtained for a single measurement in the experimental research indicates that in order to obtain the required repeatability of measurement in the range of $0.1 \div 0.2$ mm we need to perform additional repetitions of the measurement. According to formula (43), assuming the maximum permissible value of the standard deviation of the position (in the

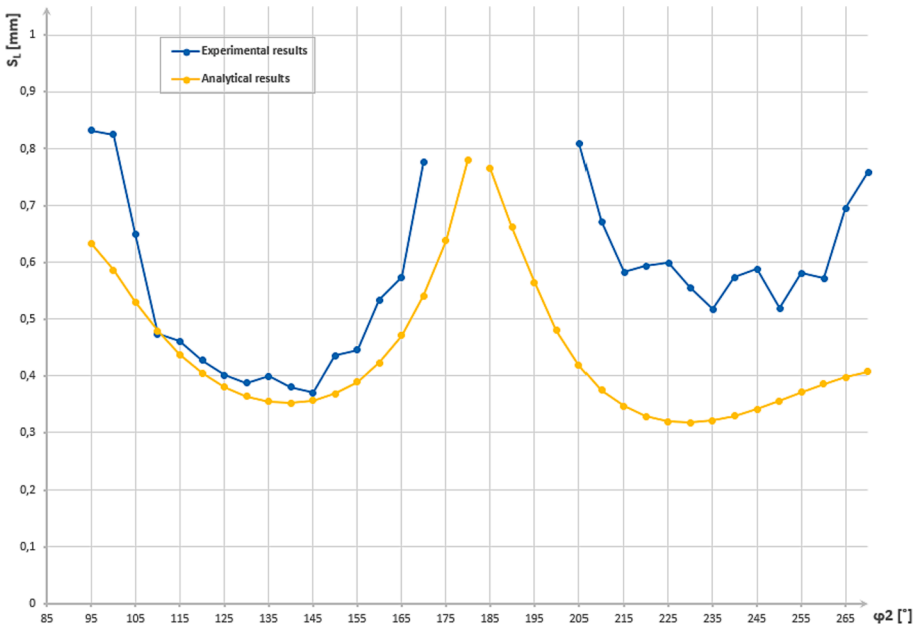

Fig. 10. Standard deviation of S_L position for variable angular position of axis 2 (φ_2) with constant angular position of axis 1 (φ_1) amounting to 295°.

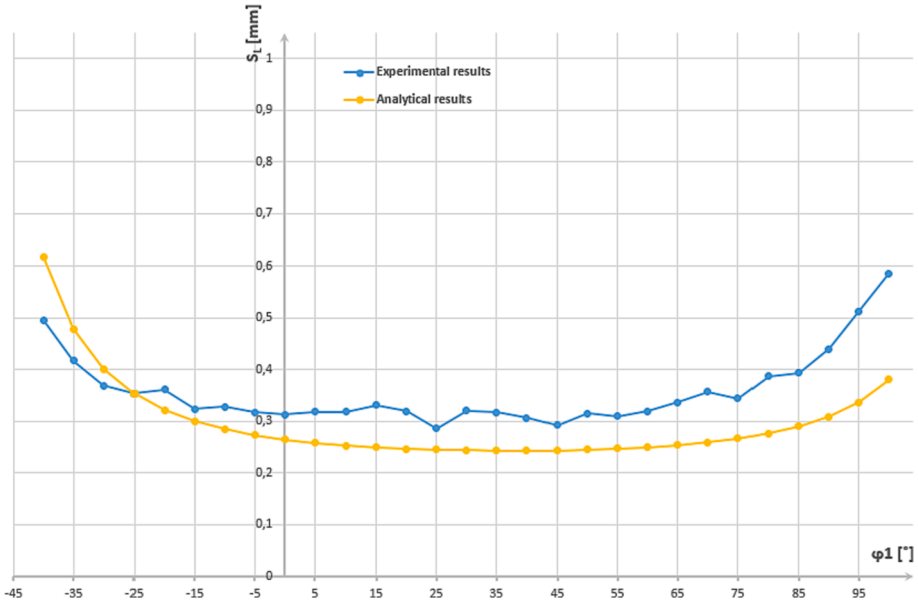

Fig. 11. Standard deviation of S_L position for variable angular position of axis 1 (φ_1) with constant angular position of axis 2 (φ_2) amounting to 180°.

working area outside the oddness points) obtained in the experimental studies, the number of n= (0.83/0.04)2 = 430 repeated measurements was calculated. In the analytical study, the number of repeated measurements was n = 380. The minimum number of repeated measurements (with the given arm configuration) determining the angles in the arm joints to achieve the required repeatability of the position and orientation measurements was assumed to be 400 measurements, so as not to unnecessarily increase the measurement time during the procedure. Due to the specificity of the use of the measuring arm - for measurement during orthopedic surgery, our goal was to define the minimum measurement time that would ensure sufficient repeatability of the measurement, despite the influence of external conditions. The time necessary to collect 400 measurements is about 4 s, during which the patient is sufficiently still. It will still be verified during the tests during actual operations. Including in the software of the measuring device a message to the user about the required time of leaving the arm stationary (in order to repeat the measurement) ensures correct operation of the device within the assumed repeatability of the measurement.

6. Summary

The described tests to determine the repeatability of the NaviFast 6D measuring arm demonstrated that for the 6 degrees of freedom position measurement method using an arm equipped only with accelerometers, the measurement is possible and the repeatability of the measurements can be determined using analytical methods. The correctness of these methods was confirmed experimentally. The dependence of the repeatability of the measurements on the position of the arm base was analyzed in detail. It was demonstrated that about 400 repetitions of measurement are necessary to obtain repeatability of measurement

averaged in the range of 0,1 ÷ 0,2 mm. It is going to last about 4 s. The range of applicability of the measuring arm in the case of approaching to the vertical of any axis of the arm joints was determined. The control program for the measuring arm includes responsive algorithms that inform the user of the required time for the device to remain stationary and messages related to alignment of the axis too close (less than 15°) to the vertical position with an indication of which axis of the arm and in which direction to correct the device position during surgery. The relatively low variability of the patient's position during the hip replacement procedure allows for the use of these arm kinematics without compromising the patient's health and with sufficient measurement repeatability to provide feedback to the operating surgeon to reduce the number of incorrectly implanted prostheses.

This measurement method, due to its relatively low cost and sufficient accuracy, can be a good alternative to many measurement devices. Further work on the measuring arm will focus on determining the impact of the accuracy of the device's construction and the impact of the way the accelerometric sensors are calibrated on the measurement accuracy.

The work was funded under Project No. POIR.01.01-00-0290/21 by the National Centre for Research and Development and financed from the budget for science in 2017-2021 as a research project under the Diamond Grant program.

CRediT authorship contribution statement

Agnieszka Kobierska: Investigation, Formal analysis, Methodology, Writing – original draft, Writing – review & editing, Validation. **Piotr Rakowski:** Investigation, Writing – original draft, Visualization. **Leszek Podsędkowski:** Supervision, Methodology, Validation.

Declaration of Competing Interest

The authors declare that they have no known competing financial interests or personal relationships that could have appeared to influence the work reported in this paper.

Data availability

Data will be made available on request.

Reference

[1] J.A. Sładek, Coordinate Metrology Accuracy of systems and measurements, Metrology Springer, 2016, DOI: 10.1007/978-3-662-48465-4_2.
[2] J. Gawlik, J. Sładek, A. Ryniewicz, M. Krawczyk, Robert Kupiec, Metrologia współrzędnościowa w inżynierii produkcji - dokładność pomiaru a dokładność wytwarzania, Inżynieria Maszyn, R. 15, z. 3, 2010.
[3] E. Jezierski, Dynamika robotów, WNT, 2006.
[4] M.W. Spong, Dynamika i sterowanie robotów, WNT, 1997.
[5] P. Rakowski, A. Kobierska, L. Podsędkowski, P. Poryzała, Accuracy and Repeatability Tests on 6D Measurement Arm, Mech. Mech. Eng. 21(2) (2017) s.425-436.
[6] Supplement 1 to the "Guide to the expression of uncertainty measurement". Propagation of distribution using Monte Carlo method, JCGM (2006).
[7] Guide to the expression of uncertainty in measurement. JCGM 2008.
[8] J. Sładek, Dokładność maszyn i pomiarów współrzędnościowych - metody wyznaczania niepewności pomiaru, Pomiary Automatyka Kontrola (12/2005.).
[9] Salma El Asmai, François Hennebelle, Thierry Coorevits, Renald Vincent, Jean-François Fontaine, Proposition of a periodic verification test for Articulated Arm Coordinate Measuring Machines using a small 3D artefact, Measurement 154 (2020) 107472.
[10] Xing Hua Li, Bo Chen, Zu Rong Qiu, The calibration and error compensation techniques for an Articulated Arm CMM with two parallel rotational axes, Measurement 46 (1) (2013) 603–609.
[11] R. Acero, A. Brau, J. Santolaria, M. Pueo, Pueo „Verification of an articulated arm coordinate measuring machine using a laser tracker as reference equipment and an indexed metrology platform", Measurement 69 (2015) 52–63.
[12] Yi Lu, Peipei Zhang, Hua Wang, Xueying Wang, Chenxin Zhao, Modeling of Measurement Space Error of AACMM, 2016 8th International Conference on Intelligent Human-Machine Systems and Cybernetics.
[13] K. Ostrowska, A. Gąska, J. Sładek, Determining the uncertainty of measurement with the use of a Virtual Coordinate Measuring Arm, 2014, DOI: 10.1007/s00170-013-5486-8.
[14] Jerzy Sładek, Ksenia Ostrowska, Adam Gąska, Adam Gąska "Modeling and identification of errors of coordinate measuring arms with the use of a metrological model", Measurement 46 (1) (2013) 667–679.
[15] Ksenia Ostrowska, Adam Gąska, Robert Kupiec, Kamila Gromczak, Paweł Wojakowski, Jerzy Sładek, Comparison of accuracy of virtual articulated arm coordinate measuring machine based on different metrological models, Measurement 133 (2019) 262–270.
[16] Fekria Romdhani, François Hennebelle, Min Ge, Patrick Juillion, Richard Coquet, Jean François Fontaine, Richard Coquet and Jean François Fontaine "Methodology for the assessment of measuring uncertainties of articulated arm coordinate measuring machines", Meas. Sci. Technol. 25 (12) (2014) 125008.
[17] Fékria Romdhani, François Hennebelle, Patrick Juillion, Richard Coquet, Jean-François FONTAINE Using of a uncertainty model of an polyarticulated coordinates measuring arm to validate the measurement in a manufacturing processsus, Procedia CIRP 33 (2015) 245 – 250 doi: 10.1016/j.procir.2015.06.044.
[18] Saeid Sepahi-Boroujeni, J.R.R. Mayer, Farbod Khameneifar, Efficient uncertainty estimation of indirectly measured geometric errors of five-axis machine tools via Monte-Carlo validated GUM framework, Precision Eng. 67 (2021) 160–171.
[19] Guanbin Gao, Wen Wang, Jianjun Zhou, Study on The Error Transfer of Articulated Arm Coordinate Measuring Machines, TELKOMNIKA 11 (2) (2013) 637–641.
[20] Xu You, Zong Zhi-jian, Gao Qun, Position uncertainty distribution for articulated arm coordinate measuring machine based on simplified definite integration, Meas. Sci. Technol. 29 (7) (2018) 075012.
[21] Andrea Zanobini, Bianca Sereni, Marcantonio Catelani, Lorenzo Ciani, Repeatability and Reproducibility techniques for the analysis of measurement systems, Measurement 86 (2016) 125–132.
[22] Dateng Zheng, Zhongyue Xiao, Xiang Xia, Multiple Measurement Models of Articulated Arm Coordinate Measuring Machines, Chin. J. Mech. Eng. 28 (5) (2015) 994–998.
[23] Yuchen Fu, Wei Fan, Huaxue Jin, Qian Chen, A new capacitance angle sensor of concentric ring multi-layer differentia, Measurement 158 (2020) 107625 DOI: 10.1016/j.measurement.2020.107625.
[24] Lisa Jogschies, Daniel Klaas, Rahel Kruppe, Johannes Rittinger, Piriya Taptimthong, Anja Wienecke, Lutz Rissing, Marc Wurz, Recent Developments of Magnetoresistive Sensors for Industrial Applications, Sensors 15 (11) (2015) 28665–28689.
[25] H. Witschnig, A. Morici, B. Schaffer, J. Zimmer, A fully monolithic integrated anisotropic magnetoresistance based angle sensor for automotive, IEEE Transducers 2013, 978-1-4673-5983-2/13].
[26] Nandapurkar Kishor Bhaskarrao, Chandrika Sreekantan Anoop,and Pranab Kumar Dutta A Novel Linearizing Signal Conditioner for Half-Bridge-Based TMR Angle Sensor, IEEE Sens. J. 21(3), FEBRUARY 1, 2021 DOI: 10.1109/JSEN.2020.3023089.
[27] Dalia Osman, Xinli Du, Wanlin Li, Yohan Noh, An Optical Joint Angle Measurement Sensor based on an Optoelectronic Sensor for Robot Manipulators, 2020 The 8th International Conference on Control, Mechatronics and Automation 978-1-7281-9210-9/20.
[28] Eduardo Palermo, Stefano Rossi, Francesca Marini, Fabrizio Patanè, Paolo Cappa, Experimental evaluation of accuracy and repeatability of a novel body-to-sensor calibration procedure for inertial sensor-based gait analysis, Measurement 52 (2014) 145–155.
[29] Manon Kok, Jeroen D. Hol, Thomas B. Schon, Using Inertial Sensors for Position and Orientation Estimation, https://doi.org/10.1561/2000000094.
[30] Norma ISO 9283 Manipulating Industrial Robots – Performance criteria and related test methods (1998).
[31] Piotr Dutka, Czynniki wpływające na dokładność i powtarzalność pozycjonowania robota przemysłowego, Pomiary Automatyka Robotyka, ISSN 1427-9126, R. 20, Nr 4/2016, 59–65, DOI: 10.14313/PAR_222/59.
[32] Jerzy Arendarski, "Niepewność pomiarów", WPW 2006.